

# Phase Transformations Contributing to the Properties of Modern Steels

H. K. D. H. Bhadeshia

University of Cambridge, Materials Science and Metallurgy  
Cambridge CB2 3QZ, U. K.

## Abstract

The role of phase transformation theory in contributing to the development of innovative steels is assessed, focusing on examples where the relationship is transparent. Virtually all of the major transformations, ranging from those which necessarily involve diffusion, to others where the change in crystal structure is achieved by a deformation, are considered.

## 1 Introduction

The plethora of structures that can be generated in steels is in part responsible for their tremendous success as engineering materials. These structures arise primarily by the solid–state transformation of austenite and lead to a huge variety of properties. Steels have evolved largely on the basis of experience and clever intuition [1–3], but an understanding of the atomic mechanisms of phase transformations combined with mathematical methods have in recent times led to few concepts which carry considerable promise [4]. In this paper we consider the essential transformations in steels and give for each case, specific examples of how they have led to some important developments.

## 2 Solid–State Transformations in Steels

The ferritic structures ( $\alpha$ ) that evolve from austenite ( $\gamma$ ) can be categorised into those whose which are dominated by strain energy given that their crystal structure is generated by a deformation of the parent lattice (displacive mechanism) and others which are closer to equilibrium because the change is achieved with the aid of diffusion (reconstructive mechanism). Amongst the displacive transformations are Widmanstätten ferrite [5], bainite [6–8], acicular ferrite [9, 10] and martensite [11–13], all of which are characterised uniquely by their plate or lath shapes and the striking

invariant–plane strain deformation caused by transformation. An important feature of this deformation is the large shear which is the dominant reason for the plate shape of the transformation product. There is no equilibrium at the transformation front; substitutional solutes do not partition between the parent and product phases.

Widmanstätten ferrite can grow at temperatures close to the paraequilibrium  $(\alpha + \gamma)/\gamma$  phase boundary, with the plates lengthen at a rate controlled by the diffusion of carbon in austenite. This diffusion does not contradict its displacive character because interstitials can migrate without affecting the shape deformation [14]. The transformation occurs at small driving forces, so that the shape change consists of two adjacent invariant–plane strains which tend to mutually accommodate and hence reduce the strain energy. This also explains the thin–wedge shape of Widmanstätten ferrite because the adjacent plates are different crystallographic variants [15]; a recent review [16] fails to account for the fact that these variants can be in similar orientation relative to the sample axes when discussing the origins of tent–shaped displacements.

Carbon must partition into the austenite during the nucleation of both Widmanstätten ferrite and bainite. Nucleation probably occurs by a process akin to the dissociation of arrays of dislocations [17]. This follows from the observation [15] that the activation energy for nucleation is directly proportional to the driving force, rather than the inverse square relationship implied by a heterophase fluctuation model of nucleation [18]. Both Widmanstätten ferrite and bainite develop from the same nucleus; bainite is stimulated if diffusionless growth is possible at the temperature where nucleation becomes possible; the nucleus otherwise evolves into Widmanstätten ferrite.

There is considerable evidence that once beyond the nucleation stage, where the surface to volume ratio dominates phenomena, bainite grows without diffusion [19–21]. Nevertheless, excess carbon is soon after transformation rejected into the residual austenite [19, 22]. The partitioned carbon may then precipitate as carbides, giving the classical upper bainitic microstructure. At somewhat lower transformation temperatures where the partitioning of carbon is slower, a proportion of the excess carbon has the opportunity to precipitate inside the bainitic ferrite. This leads to the lower bainitic microstructure [23].

Bainite ( $\alpha_b$ ) grows at temperatures where the austenite is mechanically weak and unable to elastically accommodate the shape deformation. As a result, the dislocations generated during the plastic deformation of the adjacent austenite, cause a loss of coherency at the  $\alpha_b/\gamma$  interface [24]. The growth of the bainite platelet therefore is arrested before it hits any hard obstacle such as an austenite grain boundary. Continued transformation therefore requires new platelets to form, giving rise to clusters of parallel sub–units with identical crystallographic orientation, habit plane and size [19]. These clusters are known as sheaves of bainite. Acicular ferrite is an alternative, more chaotic morphology of bainite, in which the plates are intragranularly nucleated on non–metallic inclusions and hence grow in many different directions from the nucleation site [20, 25, 26].

The possibility remains that the transition from Widmanstätten ferrite to bainite involves a gradual increase in carbon supersaturation, rather than a sudden change from paraequilibrium to diffusionless growth [27, 28]. Martensitic transformation is diffusionless, both during nucleation and during growth.

The reconstructive transformations include allotriomorphic and idiomorphic ferrite [29], and pearlite

in its various forms. It is important to appreciate that all elements, including iron, must diffuse during reconstructive transformation in order to achieve the structural change without the strains characteristic of displacive reactions [30]. None of these transformations are associated with shear strains.

A prominent feature of the eutectoid decomposition reaction which leads to the formation of pearlite is that the ferrite and carbide phases grow at a common transformation front with the austenite [31]. They are said to grow co-operatively.

The atomic mechanisms of transformation are summarised in Fig. 1; in what follows we discuss for each microstructure, how phase-transformation theory has led to the creation of new steels which are now in commercial use or at the early stages of development, focussing on a few of the achievements made during the last ten years.

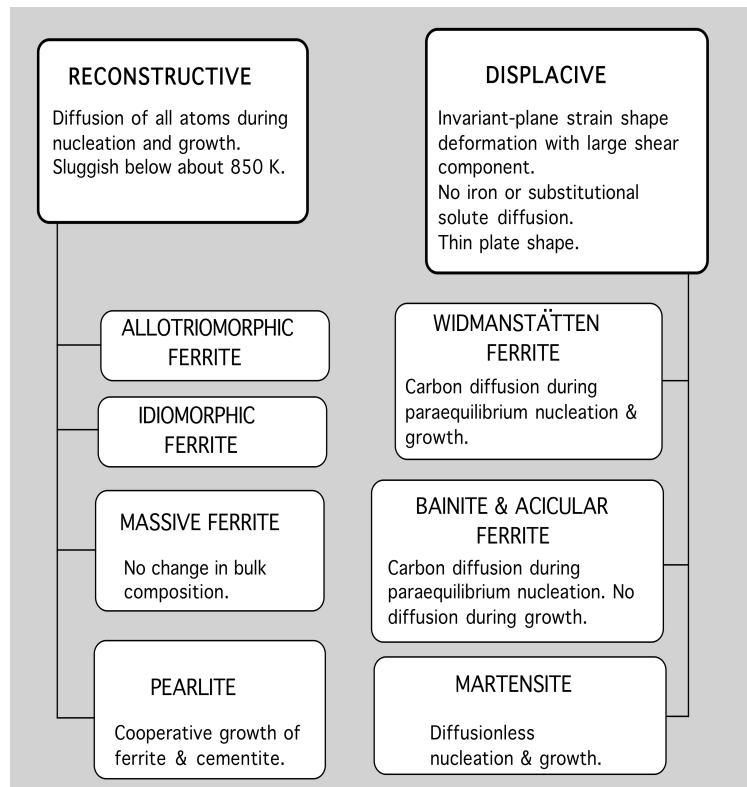


Figure 1: Characteristics of solid-state transformations in steels.

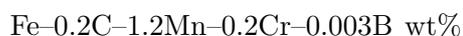
### 3 Martensitic Steels

The ground transportation industry relies on affordable materials with a high specific strength, which at the same time are able to absorb energy through controlled plastic deformation in order to ensure the integrity of passengers in the event of a crash. Steels which satisfy these criteria include the dual-phase ferrite plus martensite alloys [32] where superior ductility is achieved through the

interaction of the soft and hard phase. There are the so-called TRIP-assisted steels [33] in which solid-state phase transformation occurs under the influence of external forces, and the change in shape caused by the transformation enhances ductility via a number of mechanisms [34, 35]. The ultimate tensile strength of these alloys is in the range 500–800 MPa, and stronger steels tend to have problems with weldability [36]. Furthermore, affordable steels which are beyond this range of strength tend to be difficult to form into shape at ambient temperatures for two reasons. Components made from strong steels require larger forming loads and hence undergo greater elastic relaxation on removal from the forming press. This *springback* makes it difficult to design tools and to ensure that the finished part will fit correctly with others in the assembly. A second issue is that steels stronger than 800 MPa have yet to achieve the ductility needed to avoid cracking during complex forming operations in which the sheet contains holes prior to forming.

Martensitic steels have been invented which avoid both of these issues via a process known as *hot press forming* [40]. In one variant of the process, the steel is austenitised at a temperature in excess of 900°C, transferred hot into a press and rapidly formed into shape. Austenite at such high temperatures is weak; a Fe–0.2C–1Mn wt% steel would have a peak strength in a torsion test of 180 MPa at 900°C, decreasing to about 110 MPa at 1100°C for a strain rate of 10 s<sup>-1</sup> [37]; further results are illustrated in Fig. 2 [38]. These values are much smaller than those associated with the cold-forming of steel so the springback problem is eliminated. After shaping the steel, water is passed through the dies resulting in the steel being quenched at a rate which can be controlled between 30–100°C s<sup>-1</sup>, and the dies are opened when the temperature reaches about 100°C. The total time that the steel spends within the die is about 30 s, making this a high-productivity process. The resultant tensile strength is in excess of 1500 MPa; the elongation obtained tends to be rather low at about 6%, but a significantly higher values have not proved possible without compromising strength.

The metallurgical requirement for the steel is to end up with a fully martensitic microstructure which means that all transformations prior to the martensite-start temperature must be suppressed. This can of course be achieved by alloying, but the main application for the process is in car manufacture; a further requirement therefore is weldability, making it impossible to use large concentrations of substitutional solutes to enhance hardenability. The steels therefore typically have a chemical composition given approximately by:



The low carbon concentration in combination with the lean substitutional solute content ensures that the alloy can be joined using resistance spot welding, and the boron is there to prevent the formation of allotriomorphic ferrite by segregating to the austenite grain surfaces and rendering the boundaries less effective as heterogeneous nucleation sites [39]. To do this, the boron must be in solid solution in the austenite so it is sometimes protected against reaction with nitrogen by adding stronger nitride formers such as aluminium or titanium [40]. These principles of alloy design are well-established in the history of steels [41], but they have been applied here with considerable insight to overcome the difficulties in using the TRIP-assisted or dual-phase steels for strength beyond 800 MPa.

The ductility of the hot-press forming steels remains rather low and there is a possibility that better properties can be achieved with a bainitic microstructure. This would, however, necessitate rapid transformation rates given that the process requires transformation to be completed within

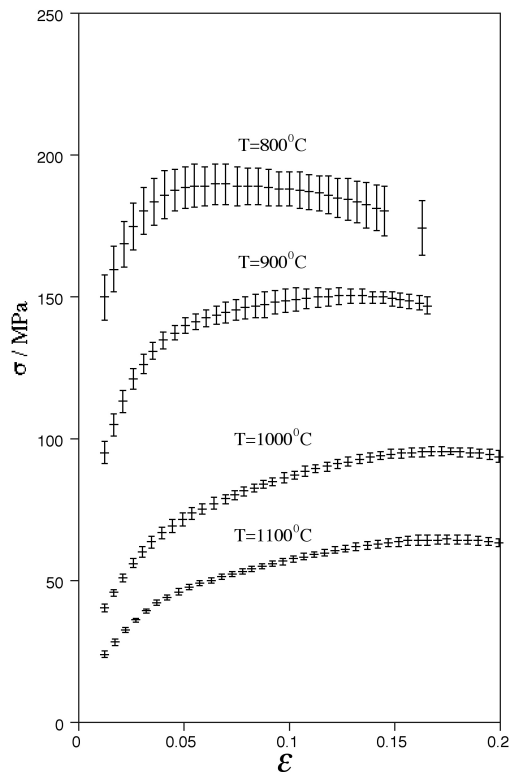


Figure 2: Stress ( $\sigma$ ) versus strain ( $\epsilon$ ) data for a Fe-0.14C-1.19Mn wt% steel for a strain rate of  $10\text{ s}^{-1}$  as a function of the test temperature [38].

a few seconds during continuous cooling after the forming is finished. Transformation rates can be accelerated by refining the austenite grain size or by increasing the magnitude of the free energy difference between the austenite and ferrite [42, 43]. However, neither of these options is likely to be sufficient to cope with the few seconds available to generate bainite and yet to achieve a strong material.

### 3.1 Flash Processing

There may nevertheless be some hope; Cola [44, 45] has claimed to have produced bainite in just 80 ms, in a process he designated *flash processing*. Steel with approximate composition Fe-0.2C-0.3Si-0.7Mn-0.5Cr-0.5Ni-0.2Mo-0.2Cu wt% was passed through an oxygen-propane fired system which applies heat directly to the strip as it passes through the equipment. The rapidly heated 1.5 mm thick strip is then quenched into water. This is a high productivity process which results in steel with a yield strength in the range 786-1487 MPa, ultimate strength 1520-1694 MPa and elongation in the range 3-10%, the most impressive combination being 1464 MPa, 1658 MPa and 10% respectively. The steels after flash processing have a mixed microstructure of bainite and martensite and would be competitive if adapted to the production process associated with hot-press forming. The details of why the bainite appears to form so rapidly are not resolved and deserve vigorous attention. It has been suggested that there is an incomplete dissolution of the cementite present in the starting microstructure and that the carbon does not have adequate time to homogenise in the austenite; the resulting carbon-depleted regions would then undergo relatively rapid transformation to bainite [45].

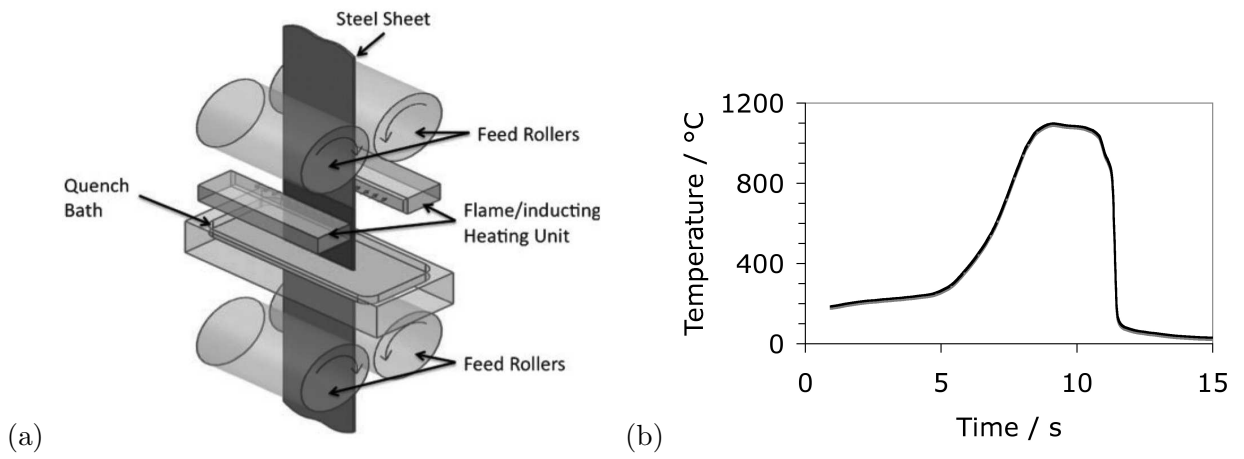


Figure 3: (a) The flash process. (b) Typical thermal profile as the sheet of steel is processed. (c) A sheaf of bainite resulting from flash processing. Information courtesy of Gary Cola [45].

### 3.2 Mechanical Stabilisation

A pressed component is not uniformly strained, so the austenite in the hot-formed state is expected to experience varying degrees of plastic deformation before it transforms into martensite. The dislocation structure associated with prior deformation can in principle stabilise the austenite and make martensitic transformation more difficult [24]. Fan et al. [40] have concluded that in hot-press forming steels the effect of the plastic strain in the austenite is to raise the martensite-start temperature ( $M_S$ ) temperature by about 5°C; this however is insignificant in comparison with the error in measuring the martensite-start temperature, which for the technique used is known to be close to  $\pm 15^\circ\text{C}$  [46]. The outcome also depends on the magnitude of the chemical driving force for transformation; if the latter is greater than the resistance to interfacial motion by dislocation debris then mechanical stabilisation will not ensue [24].

### 3.3 Martensite and Bainite as Plastic Deformations

The familiar mechanisms of plastic deformation are slip, mechanical twinning and creep. As we have seen, displacive phase transformations also cause deformation which is in detail an invariant-plane strain with a shear strain parallel to the habit plane of about 0.26, and a dilatational strain normal to the habit plane of about 0.03 [47]. The combination of the habit plane and displacement direction constitutes a deformation system, just like a slip plane and slip direction form a slip system, Table 1. The theory dealing with the interaction of this deformation system with an externally applied stress has been known for a long time [48]; a mechanical driving force results from this interaction, which adds or detracts from the chemical driving force for transformation. The stress may therefore favour the formation of certain crystallographic variants of the martensite over others whose deformations do not comply with the applied stress.

Table 1: Some habit plane and displacement directions for low-alloy steels. The indices all refer to the austenite phase and are approximate. The magnitude of the displacement, is given by  $m$ , including both the shear and the dilatational components.

Phase	Habit Plane Indices	Displacement Vector	$m$	
Martensite	(0.363 0.854 0.373)	$[\overline{0.195} \ 0.607 \ \overline{0.771}]$	0.185	[49]
Bainite	(0.325 0.778 0.537)	$[0.159 \ 0.510 \ \overline{0.845}]$	0.27	[8, 50]
Widmanstätten ferrite	(0.506 0.452 0.735)	$[\overline{0.867} \ 0.414 \ 0.277]$	0.36	[5]

In recent years, this phenomenon of *transformation plasticity* has been exploited for one of the most pernicious problems in welding technology, that of the residual stresses [51–65]. The aim is to design welding alloys which compensate for the effects of thermal contraction and stress whilst maintaining the overall mechanical performance [66, 67]. Residual stress is that which remains in an assembly at equilibrium when external fields are removed. In the context of welded structures it reduces the service load that can be tolerated, causes distortion and makes structural integrity

assessment difficult. Whereas the level of residual stress can be mitigated by heat-treatment, this is not a feasible option for large structures.

Most engineering applications involved polycrystalline steels; in such cases the shear strains on average cancel out and hence are not visible on a macroscopic scale, Fig. 4. However, when the transformation occurs under the influence of stress, certain crystallographic orientations of martensite are favoured over others and this non-random microstructure reveals the shear even in a polycrystalline austenite. Those variants which comply with the stress are favoured, and hence help to cancel the thermal contraction stresses which arise when a welded assembly cools through the transformation temperature.

As Fig. 5 illustrates, phase transformation leads to a cancelling of the state of stress in the sample, but once the transformation is exhausted, the stress builds up again as the temperature continues to decrease towards ambient. The key to designing a welding alloy which leaves the weld stress-free at ambient temperature is to lower the transformation temperature to about 200°C. This has led to welding consumables which not only have been demonstrated to reduce residual stress and distortion, but also to consequently enhance the fatigue life by impressive amounts [51–65]. This is an excellent example of how phase transformation theory has contributed to the alloy design for an essentially a practical purpose.

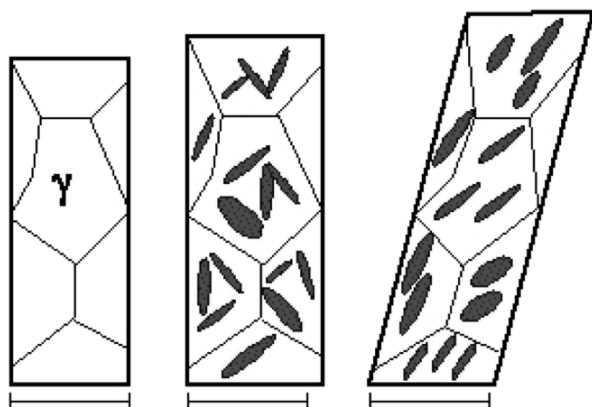


Figure 4: Plasticity due to transformation of polycrystalline austenite. When all variants of martensite precipitate it is only the volume change which is detected since the shear strains cancel out on average, but as illustrated on the right, a non-random arrangement of plates reveals both the shear and volume strains.

## 4 World’s First Bulk Nanostructured Metal

A nanostructured material is one containing an exceptionally large density of strong interfaces, not simply that which contains a minor fraction of features such as precipitates, which are small in size [69]. The search for such fine structures is driven by the potential of discovering novel mechanical properties, particularly the strength that can safely be exploited in service. It is difficult to invent such materials because any design must address three basic issues [69]:

- (i) it should ideally be possible to make samples which are large in all of its three dimensions;
- (ii) the novelty is in approaching a structural scale in polycrystalline metals which is an order of magnitude smaller.

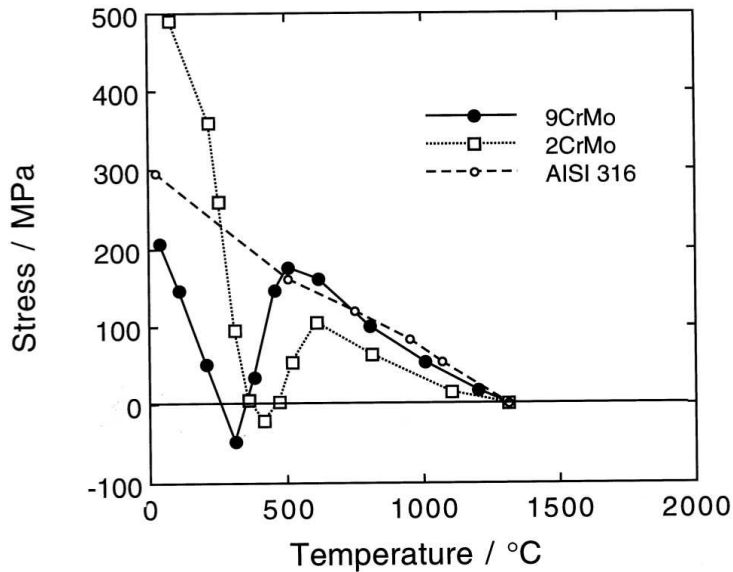


Figure 5: Development of stress as a constrained sample of austenite cools [68]. Three cases are illustrated, AISI 316 which does not transform, the 2CrMo which transforms to bainite and the 9CrMo which transforms to martensite.

(iii) The material must be cheap to produce if it is not to be limited to niche applications.

An alloy system which respects these principles, based on iron, has been invented in which it has been possible to create a high density of interfaces by heat-treatment alone [43, 70–73]. The resulting structure consists of a mixture of slender platelets of bainitic ferrite, just 20–40 nm in thickness, embedded in a matrix of carbon-enriched austenite. The rate at which this structure evolves is slow by conventional standards, but this permits components to be made which are large in all three dimensions, with uniform properties throughout. Strength and toughness combinations of 2300 MPa and  $40\text{--}50\text{ MPa m}^{\frac{1}{2}}$  respectively have been achieved. Many tens of tonnes of the material have been manufactured and the industrial process route has been established. The subject has been extensively written about [71, 74], and the phase transformation theory underpinning the invention has been documented [71, 75]. It is not, therefore, reproduced here. Suffice it to say that it represents the first nanostructured metal that can be made in huge quantities and physical dimensions on industrial processing plant. And the simple principle that enabled this achievement is to suppress the bainite-start temperature, to keep the bainite and martensite-start temperatures apart, to slow the reaction rate sufficiently to avoid recalescence [76], and to introduce a work-hardening mechanism via the strain (or stress) induced transformation of austenite during deformation. A typical micrograph is illustrated in Fig. 6.

## 5 Widmanstätten Ferrite

Although a huge amount has been written about Widmanstätten ferrite in recent years, the work has not led to innovative products, focussing instead on rather feeble kinetic models and philosophical issues. Widmanstätten ferrite has in welding alloys been regarded as something to avoid because it tends to form in aggregates of parallel, identically oriented plates growing from the austenite grain boundaries. This means that cleavage cracks can grow across the cluster of plates without much

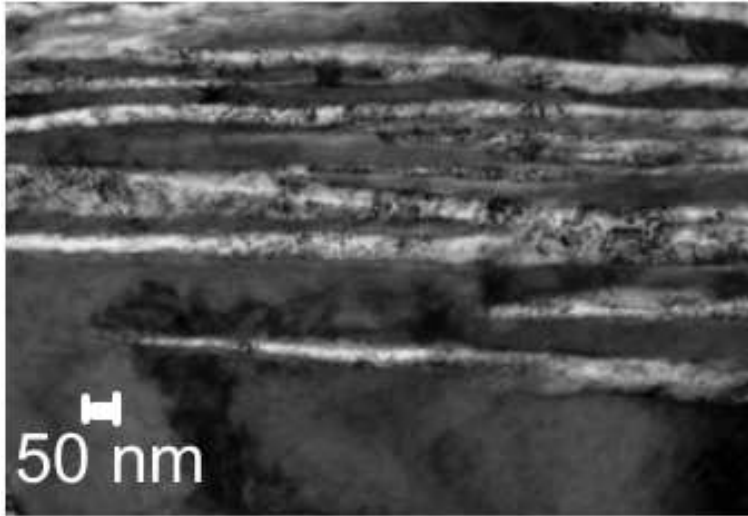


Figure 6: Fe-0.79C-1.59Si-1.94Mn-0.30Mo-1.33Cr-0.11V wt% Austenitised at 1000C for 15 min. isothermally transformed at 190C for 14 days. The width of the bainite plates (light colour) is 20–40 nm after stereological effects are taken into account. The darker phase is austenite.

effort, making the microstructure poor from a toughness point of view. There are two principles that emerge from phase transformation theory which help avoid the formation of Widmanstätten ferrite ( $\alpha_W$ ). The first is that the growth rate of the phase can be much greater than that of allotriomorphic ferrite because the plate shape allows solutes to partition to the sides of the growing plate rather than pile up ahead of the plate as is the case with allotriomorphic ferrite. The growth rates can be calculated accurately (see [77, 78] for reviews) and such calculations can be used in design [79]. The second influence is that of the austenite grain size, which favours the formation of Widmanstätten ferrite [80, 81]. This is because of its ability to outpace allotriomorphic ferrite which grows as layers at the austenite grain boundaries and hence thicken rather slowly, while the plates of  $\alpha_W$  are able to rapidly penetrate the austenite grains. The larger the austenite grains, the greater the capacity of  $\alpha_W$  to dominate the microstructure.

## 6 Allotriomorphic and Idiomorphic Ferrite

These phases dominate in the microstructures of the vast majority of steels manufactured in the world. The principles of thermomechanical processing which lead to fine ferrite grains are well established [82] and the limits to the smallest grain size that can be achieved have been established using phase transformation theory [76]. It has been shown theoretically that a grain size of allotriomorphic ferrite much smaller than  $1\ \mu\text{m}$  is unlikely in large scale–production processes [76]. With conventional controlled rolling, the transformation to ferrite occurs from deformed austenite grains, resulting in a grain size of about  $5\ \mu\text{m}$  due to the enhanced number density of nucleation sites in the pancaked austenite.

## 6.1 Dynamic Strain-Induced Transformation

A much greater degree of refinement to about  $1\ \mu\text{m}$  grain size is achieved by dynamic strain-induced transformation in which ferrite grains form during deformation in the temperature range  $Ae_3$  and  $Ar_3^1$  [83–86]. The deformation adds to the driving force for transformation, and for this reason, anything which retards the recrystallisation of austenite, for example microalloying with niobium, facilitates this process [87]. This results in extensive intragranular nucleation of (idiomorphic) ferrite. Beladi *et al.* suggest that in ordinary thermomechanical processing, the impingement of ferrite grains along the pancaked austenite grain boundaries occurs rapidly, so that the nucleation sites are saturated; subsequent transformation to consume the austenite therefore does not change the number density of ferrite grains. In contrast, when transformation occurs during deformation, the idiomorphs permit the interior of the austenite grains to contribute to the number of ferrite crystals per unit volume, thus leading to a much finer structure. Elwazri *et al.* [88] claim that the same effect is observed during deformation in the intercritical region of the phase diagram, *i.e.* at temperatures below  $Ar_3$ , but it is likely that the role of deformation diminishes as the chemical driving force for transformation increases. Dynamic strain-induced transformation is known to be most effective above  $Ar_3$ , and indeed may be most viable when the process is conducted at relatively high temperatures [89].

Fig. 7a shows typical parameters needed to obtain dynamic strain-induced transformation (DSIT) when deformation is conducted at a temperature close to  $Ae_3$  [90, 91]. A critical amount of plastic strain is necessary to initiate the effect and the equivalent strain must be high enough to achieve a large amount of strain-induced ferrite before significant grain refinement is achieved. The microstructure obtained is illustrated in Fig. 7b.

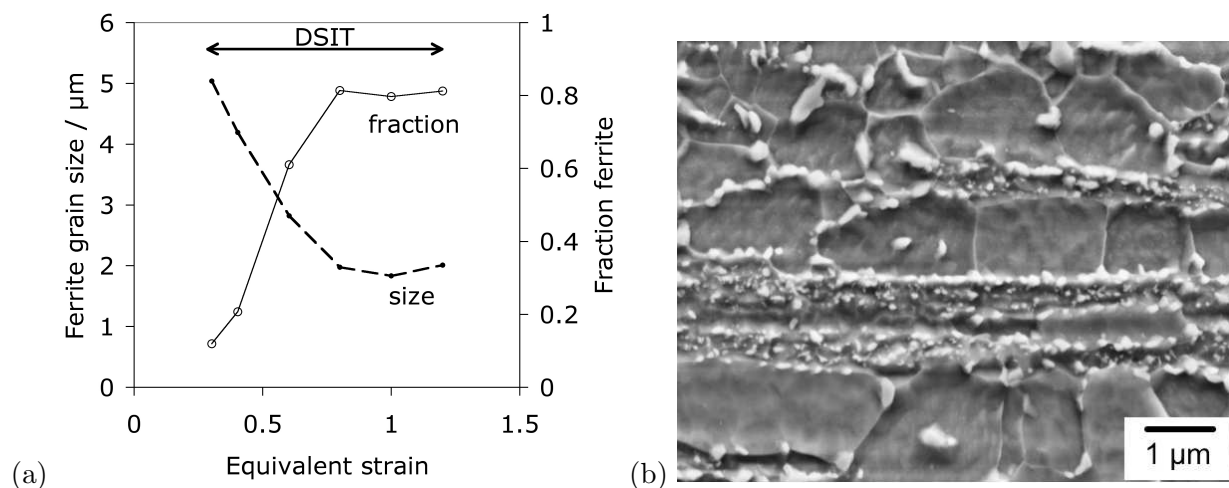


Figure 7: (a) Parameters needed to achieve dynamic strain-induced ferrite grain size refinement in Fe–0.16C–0.16Si–0.6Mn wt% steel. Data from [90]. (b) Microstructure resulting from dynamic strain-induced transformation in Fe–0.35C–0.82Mn–0.26Si–0.03Al wt%, deformed to a strain of 1.2 at  $790^\circ\text{C}$  (courtesy of H. Beladi and P. D. Hodgson).

<sup>1</sup>These stand for temperatures at which the alloy becomes fully austenitic at equilibrium and during continuous cooling at a specified rate.

## 6.2 Interphase Precipitation

The old idea of interphase precipitation [92–94], in which fine particles precipitate in rows parallel to the ferrite–austenite interface, has recently been revived [95, 96]. This is in the context of high–strength low–alloy steels used in structural applications with a yield strength in the range 400–500 MPa. The process involves the introduction of minute particles of TiC or (Ti,Mo)C particles, which result in the yield strength being elevated to  $\simeq 780$  MPa while maintaining an elongation of some 20%. Typical compositions of such steels are in the range [95]:



and the resulting microstructure is illustrated in Fig. 8.

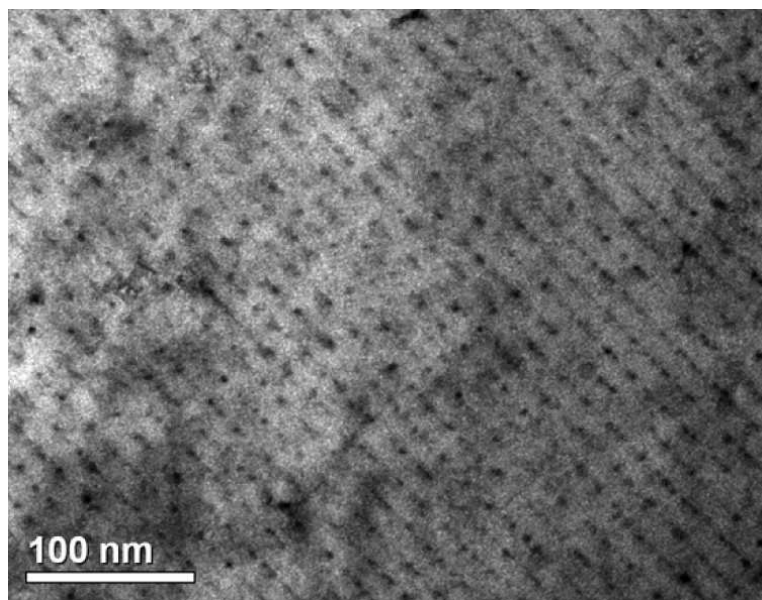


Figure 8: Regular arrays of interphase precipitates obtained by transforming a Ti and Mo containing steel at 680°C (courtesy of H. W. Yen and J. R. Yang).

## 7 Pearlite

There do not seem to have been any major developments in either the phase transformation theory relating to pearlite, or its technological applications. It is of course a significant phase in the vast majority of steels and important in its own right in steel cables and railway tracks. However, there is one interaction between theory and technology which has served the industry well.

A typical microstructure in a hot–rolled low–alloy steel is illustrated in Figure 9a [97]. There are planner patches of pearlite parallel to the rolling plane. Microstructural banding is often more pronounced in sections containing the rolling direction than in those containing the transverse direction [98, 99].

Banding occurs primarily because of the segregation of solutes in the last regions of the liquid to solidify during the cooling of steel from the molten state. The low–alloy steels which exhibit banding

typically begin solidification as  $\delta$ -ferrite so that elements such as manganese, silicon, phosphorus and sulphur are partitioned into the interdendritic regions which then solidify with a higher than average concentration of these solutes. Subsequent deformation, for example by hot-rolling, causes these regions to spread out as bands. The segregation of concern is of substitutional solute such as manganese (Figure 9b). Carbon also segregates during solidification but it diffuses rapidly as the steel cools through the austenite phase field until its chemical potential becomes uniform. The silicon concentration, which is not illustrated in Figure 9b, was also found to be in phase with the pearlite bands. Although silicon is a ferrite stabiliser, its influence on the transformation in typical steels of interest here is much smaller than that of manganese.

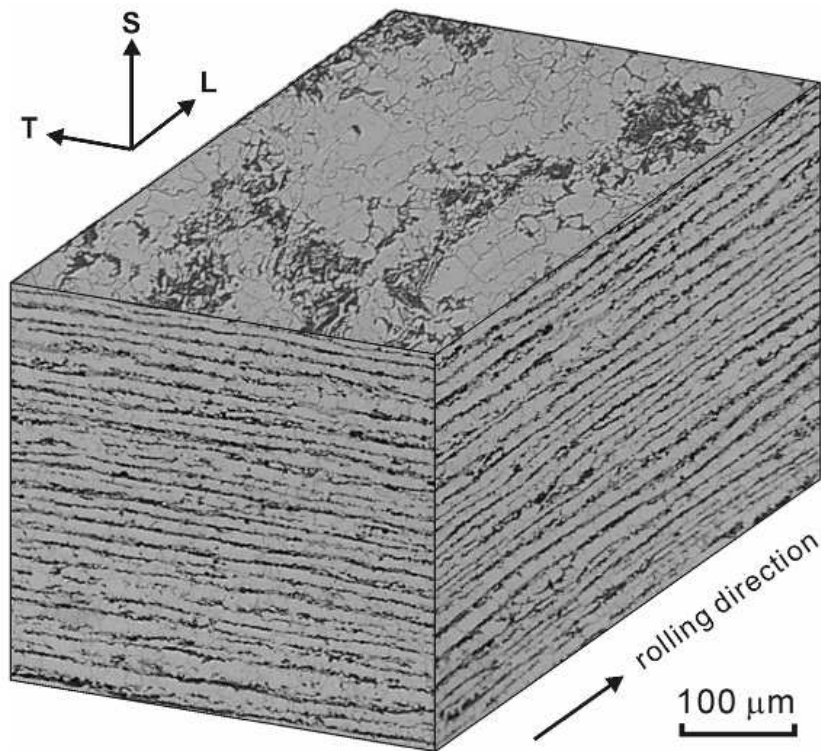
The ferrite-pearlite banding evident in Figure 9a occurs when the regions which are depleted in austenite-stabilising elements decompose into ferrite, before the transformation can occur in other areas [100]. As a result, carbon is partitioned into the adjacent substitutional-solute rich austenite, which ultimately becomes the pearlite. The microstructural banding therefore correlates with the segregation pattern and the correlation becomes more pronounced when the microstructure is generated by slow cooling. This is because larger cooling rates are associated with greater undercoolings, which permit ferrite to form even in manganese-enriched regions.

The development of microstructural banding is illustrated in Fig. 10. As pointed out previously, the highly mobile carbon homogenises during cooling through the austenite phase field. However, there are gentle variations which occur in concert with the manganese, as the carbon maintains a uniform chemical potential in the austenite. Manganese lowers the activity of carbon and hence the manganese-rich regions are associated with a somewhat higher carbon concentration [101]. The dependence of the spatial distribution of carbon on that of substitutional solute in austenite was originally thought to be the cause of banding [100]. Bastien[102], however, considered the banding to be due to the substitutional solutes and Kirkaldy [101] later showed that this is indeed the dominant effect.

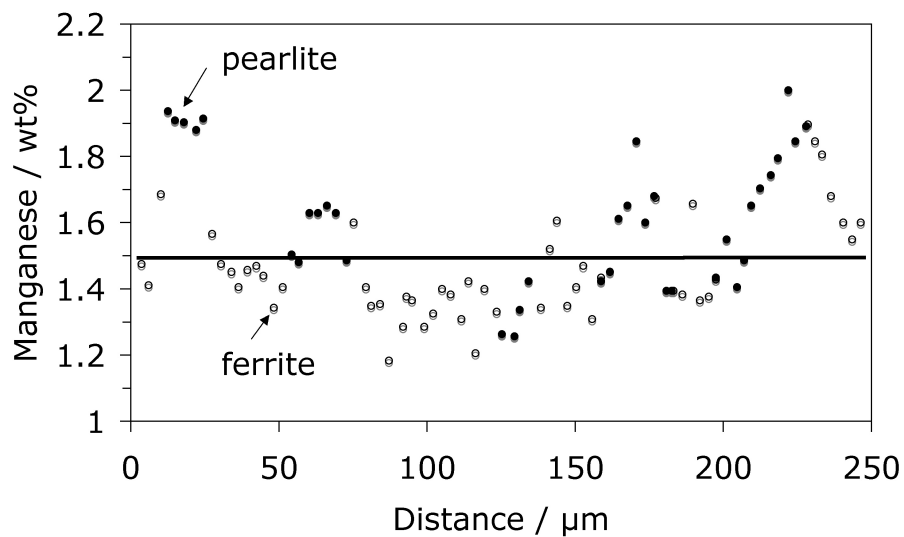
An alternative mechanism is found in steels containing large sulphur concentrations [103]. Manganese sulphides then precipitate in the regions containing a large average concentration of manganese. As a consequence, the manganese is bound in the sulphide which is surrounded by a manganese-depleted zone where ferrite forms. The ferrite partitions carbon into the adjacent zones which have a low average concentration of manganese, which transform into pearlite. The position of the ferrite bands is thus shifted into locations where the average Mn concentration is large, but where the Mn is tied up as sulphides (Fig. 11).

Because pearlite contains a lot of interfaces between its constituents, it etches dark when compared with the ferrite bands. In contrast, if the same steel is quenched to martensite then the microstructure etches uniformly, although the chemical segregation is still present. The solute-depleted regions therefore transform first into martensite, as demonstrated by Jaczak [100] who quenched the segregated steel to a temperature between  $M_S$  and  $M_F$ , then raised the temperature to beyond  $M_S$  in order to temper the partially transformed sample. On finally quenching the steel to room temperature, it consisted of bands of tempered martensite and virgin martensite, the former in the solute-depleted regions. This technique was first developed by Greninger [11].

One important difference between the ferrite-pearlite banding and the bands in fully martensitic steels is that the carbon does not partition when the martensite forms in the solute-depleted regions.



(a)



(b)

Figure 9: (a) Banding in hot-rolled ferrite-pearlite steel, Fe-0.15C-0.16Si-1.07Mn wt%. ‘S’, ‘T’ and ‘L’ stand for the short transverse, transverse and longitudinal directions respectively, in the rolling frame of reference. Courtesy of Y. Mutoh. (b) The location of pearlite relative to the manganese concentration [98].

The mechanical properties are therefore much more uniform in fully martensitic steels containing chemical segregation. The avoidance of hard, carbon-rich regions can be used to commercial advantage as follows.

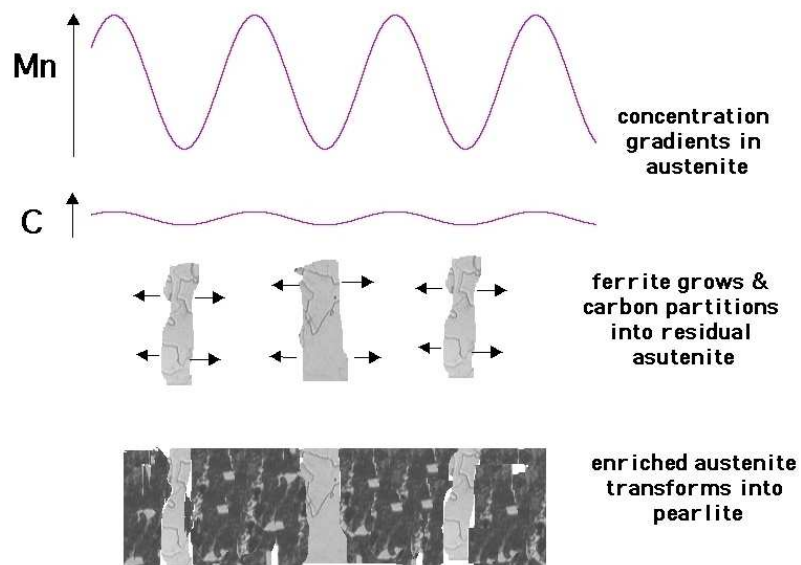


Figure 10: An illustration of the common mechanism of banding. Note that banding has irregularities so it is not entirely an accurate reflection of the chemical segregation pattern [98].

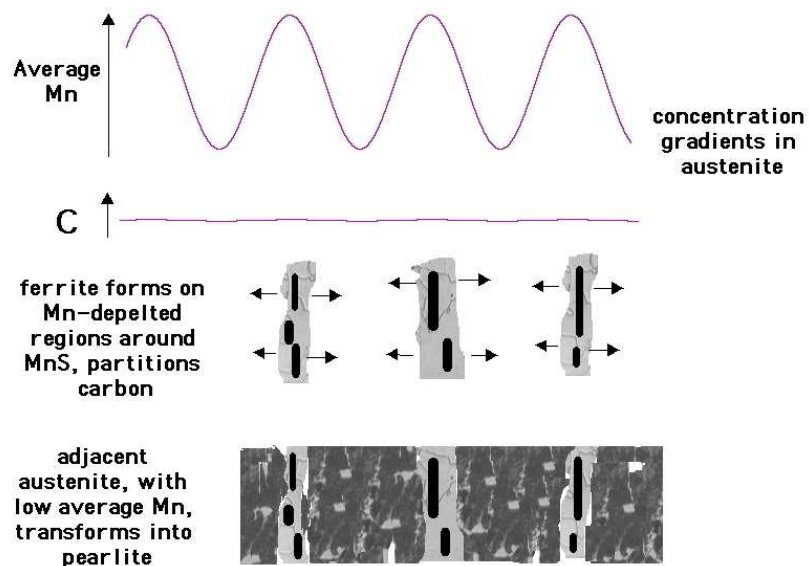


Figure 11: The mechanism of banding in steels containing substantial quantities of manganese sulphides.

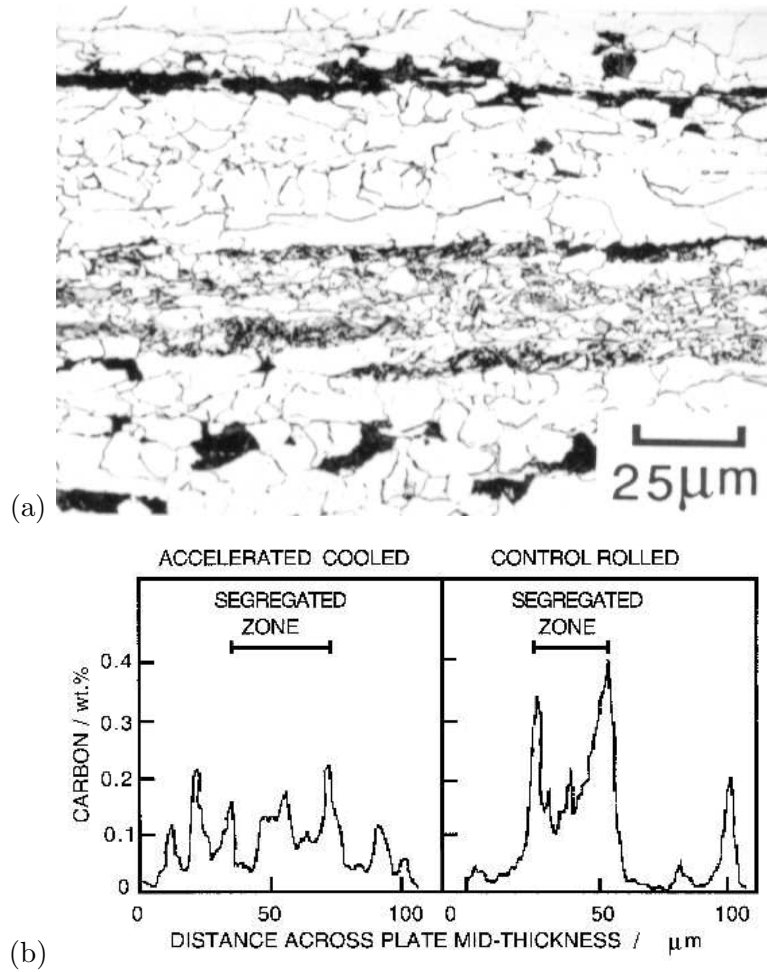


Figure 12: (a) A light micrograph illustrating the effect of chemical segregation along the mid-thickness of heavy gauge plate. (b) Distribution of carbon concentration in the segregated zone for conventional control-rolled and rapidly cooled steel plates [106].

Control-rolled steels are cast continuously so they contain pronounced chemical segregation along the mid-thickness of the plate. For example, the manganese concentration at the centre can reach twice the average value. Ferrite naturally forms first in the manganese-depleted regions; the carbon partitioned as the ferrite grows ends up in the manganese-rich regions of austenite. This exaggerates the hardenability of the manganese-rich regions which transform into bands of hard microstructure.

These bands are susceptible to hydrogen cracking. Hydrogen can be infused into the steel through corrosion reactions or other phenomena. An advantage of the accelerated cooled steels is that they are more microstructurally homogeneous (Fig. 12); this is because the ferrite and bainite form at a larger undercooling during accelerated cooling, so transformation occurs everywhere, even in the manganese-rich regions. The gross banding characteristic of ferrite-pearlite microstructures is therefore minimised or avoided altogether [104, 105]. The resulting lower hardness in the segregated zone makes the steel less susceptible to hydrogen-induced cracking. Cracking ceases to be a problem because the hardness in all regions becomes less than about 250 HV [104].

The general conclusion is that microstructures which are homogeneous, and which contain less carbon, are less susceptible to both hydrogen-induced cracking and sulphide stress-corrosion cracking. In low-carbon pipeline steels, a bainitic microstructure is found to be more resistant to these problems than one containing allotriomorphic ferrite [107].

## 8 Conclusions

I have attempted here to highlight some connections between phase transformation theory and innovation in steels. The examples chosen are selective, where a direct connection is easy to recognise. Theory and experience of course have contributed to the development of the impressive volume of steels that reliably serve society, but the relationship and significance of the different components in the creation of novel concepts is difficult to demonstrate. As such, this article is imperfect in its goal, but my hope is that it stimulates thought and further innovations.

## Acknowledgments

I am grateful to the organisers for suggesting the topic and for the invitation to participate in this conference. I also appreciate the laboratory facilities provided by Professor A. L. Greer at the University of Cambridge. Some of this work was supported by the Korea Science and Engineering Foundation under the context of the World Class University programme, project number R32-2008-000-10147-0.

## References

- [1] Anonymous. *Iron and steel: principles of manufacture, structure, composition and treatment*. Number 36 in Machinery's Reference Book. Machinery, New York, USA, 3rd edition, (1910).
- [2] F. B. Pickering. *Physical Metallurgy and the Design of Steels*. Applied Science Publishers, page 104, Essex, U.K., (1978).
- [3] F. B. Pickering. *Constitution and Properties of Steels*, pages 339–399. VCH Publishers, (1992).
- [4] H. K. D. H. Bhadeshia. Mathematical models in materials science. *Materials Science and Technology*, 24, 128–135, (2008).
- [5] J. D. Watson and P. G. McDougall. The crystallography of Widmanstätten ferrite. *Acta Metallurgica*, 21, 961–973, (1973).
- [6] T. Ko and S. A. Cottrell. The formation of bainite. *Journal of the Iron and Steel Institute*, 172, 307–313, (1952).
- [7] G. R. Srinivasan and C. M. Wayman. The crystallography of the bainite transformation. *Acta Metallurgica*, 16, 621–636, (1968).

- [8] E. Swallow and H. K. D. H. Bhadeshia. High resolution observations of displacements caused by bainitic transformation. *Materials Science and Technology*, 12, 121–125, (1996).
- [9] M. Strangwood and H. K. D. H. Bhadeshia. Mechanism of acicular ferrite formation in alloy steel weld depos. In S. A. David, editor, *Advances in Welding Technology and Science*, pages 209–213. ASM International, Materials Park, Ohio, USA, (1987).
- [10] S. S. Babu and H. K. D. H. Bhadeshia. Stress and the acicular ferrite transformations. *Materials Science and Engineering A*, A156, 1–9, (1992).
- [11] A. B. Greninger and A. R. Troiano. Kinetics of the austenite to martensite transformation in steel. *Trans. ASM*, 28, 537, (1940).
- [12] J. S. Bowles and J. K. MacKenzie. The crystallography of martensite transformations, part I. *Acta Metallurgica*, 2, 129–137, (1954).
- [13] M. S. Wechsler, D. S. Lieberman, and T. A. Read. On the theory of the formation of martensite. *Trans. AIME Journal of Metals*, 197, 1503–1515, (1953).
- [14] J. W. Christian. The origin of surface relief effects in phase transformations. In V. F. Zackay and H. I. Aaronson, editors, *Decomposition of austenite by diffusional processes*, pages 371–386. Interscience, New York, USA, (1962).
- [15] H. K. D. H. Bhadeshia. Rationalisation of shear transformations in steels. *Acta Metallurgica*, 29, 1117–1130, (1981).
- [16] M.-X. Zhang and P. M. Kelly. Crystallographic features of phase transformations in solids. *Progress in Materials Science*, 54, 1101–1170, (2009).
- [17] G. B. Olson and M. Cohen. A general mechanism of martensitic nucleation, parts i-iii. *Metallurgical Transactions A*, 7A, 1897–1923, (1976).
- [18] C. L. Magee. The nucleation of martensite. In H. I. Aaronson and V. F. Zackay, editors, *Phase Transformations*, pages 115–156. ASM International, Materials Park, Ohio, USA, (1970).
- [19] R. F. Hehemann. The bainite transformation. In H. I. Aaronson and V. F. Zackay, editors, *Phase Transformations*, pages 397–432. American Society of Materials, Materials Park, Ohio, USA, (1970).
- [20] H. K. D. H. Bhadeshia. *Bainite in Steels, 2nd edition*. Institute of Materials, London, (2001).
- [21] H. K. D. H. Bhadeshia and J. W. Christian. The bainite transformation in steels. *Metallurgical & Materials Transactions A*, 21A, 767–797, (1990).
- [22] H. K. D. H. Bhadeshia. Theoretical analysis of changes in cementite composition during the tempering of bainite. *Materials Science and Technology*, 5, 131–137, (1989).
- [23] M. Takahashi and H. K. D. H. Bhadeshia. Model for transition from upper to lower bainite. *Materials Science and Technology*, 6, 592–603, (1990).
- [24] S. Chatterjee, H. S. Wang, J. R. Yang, and H. K. D. H. Bhadeshia. Mechanical stabilisation of austenite. *Materials Science and Technology*, 22, 641–644, (2006).

- [25] Y. Ito and M. Nakanishi. Study on charpy impact properties of weld metal with SAW. *The Sumitomo Search*, 15, 42–62, (1976).
- [26] D. J. Abson and R. J. Pargeter. Factors influencing the as-deposited strength, microstructure and toughness of manual metal arc welds suitable for C–Mn steel fabrications. *International Materials Reviews*, 31, 141–194, (1986).
- [27] G. B. Olson, H. K. D. H. Bhadeshia, and M. Cohen. Coupled diffusional/displacive transformations, part ii: Solute trapping. *Metallurgical & Materials Transactions A*, 21A, 805–809, (1990).
- [28] M. Hillert. Diffusion in the growth of bainite. *Metallurgical & Materials Transactions A*, 25, 1957–1966, (1994).
- [29] C. A. Dubé, H. I. Aaronson, and R. F. Mehl. La formation de la ferrite proeutectoïde dans les aciers au carbone. *Revue de Metallurgie*, 55, 201–210, (1958).
- [30] H. K. D. H. Bhadeshia. Diffusional formation of ferrite in iron and its alloys. *Progress in Materials Science*, 29, 321–386, (1985).
- [31] M. Hillert. The formation of pearlite. In V. F. Zackay and H. I. Aaronson, editors, *Decomposition of austenite by diffusional processes*, pages 197–237. Interscience, New York, USA, (1962).
- [32] S. Hayami and T. Furukawa. A family of high-strength, cold-rolled steels. In *Microalloying '75*, volume 1, pages 78–87. Union Carbide Corporation, New York, USA, (1977).
- [33] O. Matsumura, Y. Sakuma, and H. Takechi. Enhancement of elongation by retained austenite in intercritical annealed 0.4C-1.5Si-0.8Mn steel. *Transactions of the Iron and Steel Institute of Japan*, 27, 570–579, (1987).
- [34] W. W. Gerberich, G. Thomas, E. R. Parker, and V. F. Zackay. Metastable austenites: decomposition and strength. In *Second International Conference on Strength of Metals and Alloys*, pages 894–899. ASM International, Ohio, USA, (1970).
- [35] H. K. D. H. Bhadeshia. TRIP-assisted steels? *ISIJ International*, 42, 1059–1060, (2002).
- [36] M. I. Khan, M. L. Kuntz, and Y. Zhou. Effects of weld microstructure on static and impact performance of resistance spot welded joints in advanced high strength steels. *Science and Technology of Welding and Joining*, 13, 294–304, (2008).
- [37] L. X. Kong, P. D. Hodgson, and D. C. Collinson. Modelling the effect of carbon content on hot strength of steels using a modified artificial neural network. *ISIJ International*, 38, 1121–1130, (1998).
- [38] V. Narayan, R. Abad, B. Lopez, H. K. D. H. Bhadeshia, and D. J. C. MacKay. Estimation of hot torsion stress strain curves in iron alloys using a neural network analysis. *ISIJ International*, 39, 999–1005, (1999).
- [39] A. Brownrigg. Boron in steel - a literature review. *The Journal of the Australasian Institute of Metals*, 18, 124–136, (1973).

- [40] D. W. Fan, H. S. Kim, and B. C. De Cooman. Review of the physical metallurgy related to hot press forming of advanced high strength steel. *Steel Research International*, 80, 241–248, (2009).
- [41] F. B. Pickering. *Physical Metallurgy and the Design of Steels*. Applied Science Publishers, Essex, U. K., (1978).
- [42] H. I. Aaronson, H. A. Domian, and G. M. Pound. Partitioning of alloying elements between austenite and proeutectoid ferrite and bainite. *TMS-AIME*, 236, 781–796, (1966).
- [43] C. Garcia-Mateo, F. G. Caballero, and H. K. D. H. Bhadeshia. Acceleration of low-temperature bainite. *ISIJ International*, 43, 1821–1825, (2003).
- [44] G. M. Cola Jr. Properties of bainite nucleated by water quenching in 80 ms. In T. Furuhashi and K. Tsuzaki, editors, *1st International Symposium on Steel Science*, pages 187–190. Iron and Steel Institute of Japan, Tokyo, Japan, (2007).
- [45] T. Lolla, G. Coal, B. Narayanan, B. Alexandrov, and S. S. Babu. Development of rapid heating and cooling (flash processing) process to produce advanced high strength steel microstructures. *Materials Science and Technology*, 14, DOI 10.1179/17428409X433813, (2009).
- [46] H.-S. Yang and H. K. D. H. Bhadeshia. Uncertainties in the dilatometric determination of the martensite-start temperature. *Materials Science and Technology*, 23, 556–560, (2007).
- [47] J. W. Christian. Deformation by moving interfaces. *Metallurgical Transactions A*, 13, 509–538, (1982).
- [48] J. R. Patel and M. Cohen. Criterion for the action of applied stress in the martensitic transformation. *Acta Metallurgica*, 1, 531–538, (1953).
- [49] D. P. Dunne and C. M. Wayman. An assessment of the double shear theory as applied to ferrous martensitic transformations. *Acta Metallurgica*, 19, 425–438, (1971).
- [50] Y. Ohmori. The crystallography of the lower bainite transformation in a plain carbon steel. *Trans. ISIJ*, 11, 95–101, (1971).
- [51] A. Ohta, N. Suzuki, Y. Maeda, K. Hiraoka, and T. Nakamura. Superior fatigue crack growth properties in newly developed weld metal. *International Journal of Fatigue*, 21, S113–S118, (1999).
- [52] A. Ohta, O. Watanabe, K. Matsuoka, C. Shiga, S. Nishijima, Y. Maeda, N. Suzuki, and T. Kubo. Fatigue strength improvement by using newly developed low transformation temperature welding material. *Welding in the World*, 43, 38–42, (1999).
- [53] A. Ohta, N. Suzuki, and Y. Maeda. In A. Meike, editor, *Properties of Complex Inorganic Solids 2*, pages 401–408. Kluwer Academic/Plenum Publishers, (2000).
- [54] P. J. Withers and H. K. D. H. Bhadeshia. Residual stress part 1 - measurement techniques. *Materials Science and Technology*, 17, 355–365, (2001).
- [55] P. J. Withers and H. K. D. H. Bhadeshia. Residual stress part 2 - nature and origins. *Materials Science and Technology*, 17, 366–375, (2001).

- [56] A. Ohta, K. Matsuoka, N. T. Nguyen, Y. Maeda, and N. Suzuki. Fatigue strength improvement of lap welded joints of thin steel plate using low transformation temperature welding wire. *Welding Journal, Research Supplement*, 82, 77s–83s, (2003).
- [57] J. Eckerlid, T. Nilsson, and L. Karlsson. Fatigue properties of longitudinal attachments welded using low transformation temperature filler. *Science and Technology of Welding and Joining*, 8, 353–359, (2003).
- [58] H. Lixing, W. Dongpo, W. Wenxian, and Y. Tainjin. Ultrasonic peening and low transformation temperature electrodes used for improving the fatigue strength of welded joints. *Welding in the World*, 48, 34–39, (2004).
- [59] S. Zenitani, N. Hayakawa, J. Yamamoto, K. Hiraoka, Y. Morikage, T. Yauda, and K. Amano. Development of new low transformation temperature welding consumable to prevent cold cracking in high strength steel welds. *Science and Technology of Welding and Joining*, 12, 516–522, (2007).
- [60] J. A. Francis, H. J. Stone, S. Kundu, R. B. Rogge, H. K. D. H. Bhadeshia, P. J. Withers, and L. Karlsson. Transformation temperatures and welding residual stresses in ferritic steels. In *Proceedings of PVP2007, ASME Pressure Vessels and Piping Division Conference*, pages 1–8. American Society of Mechanical Engineers, ASME, San Antonio, Texas, (2007).
- [61] Ph. P. Darcis, H. Katsumoto, M. C. Payares-Asprino, S. Liu, and T. A. Siewert. Cruciform fillet welded joint fatigue strength improvements by weld metal phase transformations. *Fatigue and Fracture of Engineering Materials and Structures*, 31, 125–136, (2008).
- [62] M. C. Payares-Asprino, H. Katsumoto, and S. Liu. Effect of martensite start and finish temperature on residual stress development in structural steel welds. *Welding Journal, Research Supplement*, 87, 279s–289s, (2008).
- [63] H. Dai, J. A. Francis, H. J. Stone, H. K. D. H. Bhadeshia, and P. J. Withers. Characterising phase transformations and their effects on ferritic weld residual stresses with X-rays and neutrons. *Metallurgical & Materials Transactions A*, 39, 3070–3078, (2008).
- [64] Y. Mikami, Y. Morikage, M. Mochizuki, and M. Toyoda. Angular distortion of fillet welded T joint using low transformation temperature welding wire. *Science and Technology of Welding and Joining*, 14, 97–105, (2009).
- [65] A. A. Shirzadi, H. K. D. H. Bhadeshia, L. Karlsson, and P. J. Withers. Stainless steel weld metal designed to mitigate residual stresses. *Science and Technology of Welding and Joining*, 14, 559–565, (2009).
- [66] H. K. D. H. Bhadeshia. Strong ferritic-steel welds. *Materials Science Forum*, 539–543, 6–11, (2007).
- [67] H. K. D. H. Bhadeshia. Frontiers in the modelling of steel weld deposits. *Journal of the Japan Welding Society*, 76, 26–32, (2007).
- [68] W. K. C. Jones and P. J. Alberry. A model for stress accumulation in steels during welding. *Metals Technology*, 11, 557–566, (1977).
- [69] H. K. D. H. Bhadeshia. Nanostructured bainite. *Proceedings of the Royal Society of London A*, page in press, (2010).

- [70] F. G. Caballero, H. K. D. H. Bhadeshia, K. J. A. Mawella, D. G. Jones, and P. Brown. Very strong, low-temperature bainite. *Materials Science and Technology*, 18, 279–284, (2002).
- [71] F. G. Caballero and H. K. D. H. Bhadeshia. Very strong bainite. *Current Opinion in Solid State and Materials Science*, 8, 251–257, (2004).
- [72] C. Garcia-Mateo, F. G. Caballero, and H. K. D. H. Bhadeshia. Development of hard bainite. *ISIJ International*, 43, 1238–1243, (2003).
- [73] M. Peet, S. S. Babu, M. K. Miller, and H. K. D. H. Bhadeshia. Three-dimensional atom probe analysis of carbon distribution in low-temperature bainite. *Scripta Materialia*, 50, 1277–1281, (2004).
- [74] H. K. D. H. Bhadeshia. Large chunks of very strong steel. *Materials Science and Technology*, 21, 1293–1302, (2005).
- [75] H. K. D. H. Bhadeshia. Hard bainite. In J. M. Howe, D. E. Laughlin, J. K. Lee, U. Dahmen, and W. A. Soffa, editors, *Solid-Solid Phase Transformations, TMS-AIME, Warrendale, USA*, volume 1, pages 469–484. TMS-AIME, Warrendale, Pennsylvania, USA, (2005).
- [76] T. Yokota, C. Garcia-Mateo, and H. K. D. H. Bhadeshia. Formation of nanostructured steel by phase transformation. *Scripta Materialia*, 51, 767–770, (2004).
- [77] R. Trivedi. Volume diffusion-controlled growth kinetics and mechanisms in binary alloys. In H. I. Aaronson, editor, *Solid-Solid Phase Transformations*, pages 477–502. TMS-AIME, Warrendale, Pennsylvania, USA, (1982).
- [78] H. K. D. H. Bhadeshia. Critical assessment: Diffusion-controlled growth of ferrite plates in plain carbon steels. *Materials Science and Technology*, 1, 497–504, (1985).
- [79] H. K. D. H. Bhadeshia, L.-E. Svensson, and B. Grefott. Model for the development of microstructure in low alloy steel (Fe-Mn-Si-C) weld deposits. *Acta Metallurgica*, 33, 1271–1283, (1985).
- [80] R. L. Bodnar and S. S. Hansen. Effects of austenite grain size and cooling rate on Widmanstätten ferrite formation in low alloy steels. *Metallurgical & Materials Transactions A*, 25A, 665–675, (1994).
- [81] S. Jones and H. K. D. H. Bhadeshia. Kinetics of the simultaneous decomposition of austenite into several transformation products. *Acta Materialia*, 45, 2911–2920, (1997).
- [82] G. R. Speich, L. J. Cuddy, C. R. Gordon, and A. J. DeArdo. Formation of ferrite from control-rolled austenite. In A. R. Marder and J. I. Goldstein, editors, *Phase Transformations in Ferrous Alloys*, pages 341–389. TMS-AIME, Warrendale, Pennsylvania, USA, (1984).
- [83] P. J. Hurley, G. L. Kelly, and P. D. Hodgson. Ultrafine ferrite formation during hot strip rolling. *Materials Science and Technology*, 16, 1273–1276, (2000).
- [84] P. J. Hurley and P. D. Hodgson. Effect of process variables on formation of dynamic strain induced ultrafine ferrite during hot torsion testing. *Materials Science and Technology*, 17, 1360–1368, (2001).

- [85] H. Beladi, G. L. Kelly, and P. D. Hodgson. Ultrafine grained structure formation in steels using dynamic strain induced transformation processing. *International Materials Reviews*, 52, 14–28, (2007).
- [86] A. Shokouhi and P. D. Hodgson. Effect of transformation mechanism (static or dynamic) on final ferrite grain size. *Materials Science and Technology*, 25, 29–34, (2009).
- [87] P. R. Rios, S. de Bott, D. B. Santos, T. M. F. de Melo, and J. L. Ferreira. Effect of Nb on dynamic strain induced austenite to ferrite transformation. *Materials Science and Technology*, 23, 417–422, (2007).
- [88] A. M. Elwazri, P. Wanjaraz, R. Varano, G. R. Stewart, S. Yue, and J. J. Jones. Microstructure and mechanical properties of ultrafine-grained steel. In *Materials Science and Technology Conference and Exhibition*, pages 1764–1775. TMS–AIME, Materials Park, Ohio, USA, (2008).
- [89] J. L. Ferreira, T. M. F. de Melo, I. S. Bott, D. B. Santos, and P. R. Rios. Influence of thermo-mechanical parameters on the competition between dynamic recrystallization and dynamic strain induced transformation in C–Mn and C–Mn–Nb steels deformed by hot torsion. *ISIJ International*, 47, 1638–1646, (2007).
- [90] H. Beladi, G. L. Kelly, and P. D. Hodgson. Formation of ultrafine grained structure in plain carbon steels through thermomechanical processing. *Materials Transactions*, 45, 2214–2218, (2004).
- [91] P. D. Hodgson, H. Beladi, and M. R. Barnett. Grain refinement in steels through thermomechanical processing. *Materials Science Forum*, 500-501, 39–48, (2005).
- [92] W. B. Morrison. The influence of small niobium additions on the properties of carbon–manganese steels. *Journal of the Iron and Steel Institute*, 201, 317–325, (1967).
- [93] R. W. K. Honeycombe. Transformation from austenite in alloy steels. *Metallurgical Transactions A*, 7, 915–936, (1976).
- [94] W. B. Morrison. Microalloy steels – the beginning. *Materials Science and Technology*, 25, 1066–1073, (2009).
- [95] Y. Funakawa, T. Shiozaki, K. Tomita, Y. Yamamoto, and E. Maeda. Development of high strength hot-rolled sheet steel consisting of ferrite and nanometer-sized carbides. *ISIJ International*, 44, 1945–1951, (2004).
- [96] C.Y. Chen, H.W. Yen, F.H. Kao, W.C. Li, C.Y. Huang, J.R. Yang, and S.H. Wang. Precipitation hardening of high-strength low-alloy steels by nanometer-sized carbides. *Materials Science and Engineering: A*, 499, 162 – 166, (2009).
- [97] A. A. Korda, Y. Mutoh, Y. Miyashita, T. Sadasue, and S. L. Manan. In situ observation of fatigue crack retardation in banded ferrite–pearlite microstructure due to crack branching. *Scripta Materialia*, 8, 1835–1840, (2006).
- [98] S. W. Thompson and P. R. Howell. Factors influencing ferrite/pearlite banding and origin of large pearlite nodules in a hypoeutectoid plate steel. *Materials Science and Technology*, 8, 777–784, (1992).

- [99] D. Chae, D. A. Koss, A. L. Wilson, and P. R. Howell. Effect of microstructural banding on failure initiation of HY-100 steel. *Metallurgical & Materials Transactions A*, 31A, 995–1005, (2000).
- [100] C. F. Jataczak, D. J. Girardi, and E S Rowland. On banding in steel. *Trans. ASM*, 48, 279–305, (1956).
- [101] J. S. Kirkaldy, J. von Destinon-Forstmann, and R. J. Brigham. Simulation of banding in steels. *Canadian Metallurgical Quarterly*, 59, 59–81, (1962).
- [102] P. G. Bastien. The mechanism of formation of banded structures. *Journal of the Iron and Steel Institute*, 187, 281–291, (1957).
- [103] J. S. Kirkaldy, R. J. Brigham, H. A. Domian, and R. G. Ward. A study of banding in Skelp by electron-probe microanalysis. *Canadian Metallurgical Quarterly*, 2, 233–241, (1963).
- [104] H. Tamehiro, R. Habu, N. Yamada, H. Matsuda, and M. Nagumo. Properties of large diameter line pipe steel produced by accelerated cooling after controlled rolling. In P. D. Southwick, editor, *Accelerated Cooling of Steel*, pages 401–414, (1985).
- [105] M. K. Graf, H. G. Hillenbrand, and P. A. Peters. Accelerated cooling of plate for high-strength large-diameter pipe. In P. D. Southwick, editor, *Accelerated Cooling of Steel, TMS AIME*, pages 165–180, (1985).
- [106] H. Tamehiro, T. Takeda, S. Matsuda, K. Yamamoto, and N. Okumura. Effect of accelerated cooling after controlled rolling on hydrogen induced cracking resistance of line pipe steel. *Trans. ISIJ*, 25, 982–988, (1985).
- [107] M.-C. Zhao, Y.-Y. Shan, F. R. Xiao, K. Yang, and Y. H. Li. Investigation on the H<sub>2</sub>S-resistant behaviors of acicular ferrite and ultrafine ferrite. *Materials Letters*, 57, 141–145, (2002).